SPE 62902

Cross-Discipline Integration in Reservoir Modeling: The Impact on Fluid Flow Simulation and Reservoir Management

Hisham M. Al Qassab, SPE, John Fitzmaurice, Zaki A. Al-Ali, SPE, Mohammed A. Al-Khalifa, G. A. Aktas, Saudi Aramco, and Paul W. Glover, U. of Aberdeen

This paper was prepared for presentation at the 2000 SPE Annual Technical Conference and Exhibition held in Dallas, Texas, 1–4 October 2000.

Abstract

A new technique is developed for modeling 3D permeability distributions. The technique integrates all available data into a fluid flow simulation model. The integrated modeling process honors the essential aspects of the established reservoir descriptions as well as the geological facies model and engineering data. The added value of data integration of the fluid flow simulation is illustrated by the improved accuracy of the resulting well performance predictions and the decrease in time requirements for reservoir modeling history matching.

The technique utilizes diverse data at different scales to condition reservoir models of facies, porosity, and permeability. Such data includes 3D seismic, well logs, core measurements, geologic facies distribution, flow meter logs, and pressure buildup tests. The model building process explicitly accounts for the difference in scale of the various measurements. The model calculates the porosity, facies, and permeability in the inter well volume using geostatistical techniques that are constrained by seismic impedance derived from the 3D seismic data. The use of engineering data in the permeability modeling constrains the results and decreases the history matching time requirements.

A case study demonstrates the modeling technique. A reservoir model is developed for the Unayzah Formation in the Hawtah Field of Saudi Arabia. The Unayzah is a highly stratified clastic reservoir in a mixed fluvial and eolian depositional environment. Data integration provided more realistic reservoir model for this complex geologic setting than the conventional approach. Specifically, the integrated approach provide a reservoir model that captured the complex and highly stratified nature of the lithological units. Fluid flow simulation was carried out for both the new integrated reservoir model and the conventional reservoir model. Results show tremendous savings in history matching time and more accurate results for use in reservoir management production strategies when applying the new technique.

Introduction

At the present time there is an increasing demand for detailed geological numerical models which incorporate all available data into reservoir characterization studies for the purpose of fluid flow simulation. Conventional modeling techniques, which lack the ability to quantitatively integrate data, tend to produce homogenous results of reservoir properties in the inter-well regions. These models, when fed into reservoir simulations for performance predictions, may generate biased and unreliable results. This necessitates the development of an method that integrates all available data, despite differences in scale, improving the predictive power of the models and making it possible to obtain quicker production history matching from the reservoir simulation.

One of the primary reasons for using geostatistics in the reservoir modeling process is data integration. That is, it allows the incorporation of diverse data of varying scale. This can include very descriptive data, such as conceptual geologic interpretations, or measurements such as 3D seismic time traces, their derivatives, and the resulting interpretations. Geostatistical tools can use data such as 3D seismic to directly or indirectly contribute to the modeling of the inter-well regions. This may provide significant risk reduction in reservoir development and management.

This paper presents a geostatistical methodology that has been adopted for integrating geophysical, geological, and engineering data in reservoir modeling. The Hawtah Field, located in the central part of Saudi Arabia (Fig. 1), has been chosen to demonstrate the approach. Hawtah is a recently developed field with a wealth of modern geological, petrophysical, geophysical, and production data. Incorporating all of this information into the reservoir model exceeded the capability of conventional numerical models.

Depositional facies maps representing geologic environments were generated using core-calibrated

electrofacies from well logs. The facies model was generated by geostatistical interpolation of the electrofacies logs using Sequential Indicator Simulation (SIS).

A stochastic seismic post-stack amplitude inversion was carried out to produce a high-resolution (well log scale) acoustic impedance model. A porosity model was then generated using both the SIS facies model and the acoustic impedance model as soft data. Finally, a permeability model was constructed, which is conditioned to Kh from pressure buildups allocated by flow meter profiles, core data, and the resulting porosity model.

Reservoir properties of this integrated model were then input to the reservoir simulation and the history-match results compared with those of the conventional models. Histograms of pressure match, CPU versus time steps, and error analysis plots are displayed for comparative analysis for flow predictions using both models.

Stratigraphic and Reservoir Architecture of Unayzah Reservoirs In Hawtah Field

The Unayzah Reservoirs in the Hawtah Field are composed largely of rocks of continental origin, organized in a highly complex fashion. Untangling the complex facies architecture of these reservoirs has required passing through several evolutionary stages. Earlier conceptions advocated a complex picture with a relatively random distribution of reservoir and non-reservoir facies distributions. However, more recent detailed stratigraphic and sedimentological studies suggest that the rock architecture of the Unayzah reservoirs is in fact much better organized than originally believed. Furthermore, a sequence stratigraphic scheme can be applied in order to allow a better understanding of reservoir prediction and connectivity for the most part of the reservoirs.

The Unayzah Reservoirs in the Hawtah Field can be divided into three major units; the basal Lower Unayzah (B), the middle Upper Unayzah (A), and locally well-developed basal Khuff clastics on top (Fig. 2).

The Lower Unayzah (B) and underlying pre-Unayzah Sequences represent sedimentary successions filling a structural irregular topography (post orogenic early rift) following the Hercynian Orogeny. These sediments are composed of dry and wet alluvial fan and also associated glacio-fluvial deposits.

The sediments of Unayzah-A signal a major shift in depositional and tectonic styles from the underlying Unayzah-B sandstones. The principal reservoir unit of the Unayzah A can be divided into 5 major aggradational cycles which are laterally correlatable and can be further subdivided into 13 sequences. Individual cycles show upward-cleaning characteristics, most commonly starting with trangressive lacustrine and associated sabkha and interdune facies in the lower parts, followed by aeolian, and locally by ephemeral fluvial channel deposits in variable proportions. These cycles represent overall upward-drying sequences developed in response to fluctuating climatic conditions probably caused by large scale cyclic orbital variations. Lake transgressions are attributed to the periods of deglaciation of gradually-diminishing icecaps. Thickening of cycles along the flanks of field is attributed to ongoing subtle differential tectonic subsidence.

The youngest reservoir unit, the Basal Khuff unit is characterized in the study area by localized lowstand incised valley fill sandstones which form locally prominent high quality reservoir bodies.

This brings the total number of stratigraphic sequences/zones to 15 zones which will be used for the purpose of reservoir modeling.

Unayzah Depositional Facies Maps and Model

The goal of building facies model in any reservoir characterization study is to identify the spatial distribution of rock types that control fluid flow behavior. However, one difficulty in any study including this one is the availability and quality of core data that define rock or facies types. Therefore, we adopted a two-fold method. First, we identify facies types and associations in terms of depositional environment from cored wells so that geological characteristics can be explained in details that are geologically sound. Once the facies were identified at cored wells, they were extended to non-cored wells which have well logs available. The output from this method was a foot-by-foot determination of depositional environment facies types in each well in the Hawtah Field. Table 1 shows a description of each of the depositional environment facies associations.

Facies maps were hand-drawn by the geologist for each of the 13 zones within Unayzah-A Reservoir. This was accomplished by simply assigning a facies type for each well for a given zone. This facies type represents the facies with the highest proportion for a given zone. A facies value was then plotted for every well location and directional data from bore hole image logs in the form of a trend was placed next to the facies type. This map was then hand contoured honoring the facies type, directional indication from well image logs, and the regional depositional characteristics of Unayzah Formation (Fig. 3).

These hand-drawn maps were then used to build a 3D environment of depositional facies model for the entire reservoir. This was done by treating each facies type from the hand-drawn facies maps as a region and then separately distributing facies available at wells within that region using a categorical geostatistical algorithm for facies namely Sequential Indicator Simulation (SIS). Fig. 4 shows comparison between facies maps for a selected zone and the resulting 3D model.

Unayzah Petrophysical Rock Model

Examination of reservoir properties such as porosity and permeability for the different depositional environment facies indicated substantial overlap between them, as clearly seen in Fig. 5. Therefore, it was concluded that depositional environment facies can not be used alone to determine reservoir flow units for the purpose of this study. As a result, an in-house cluster analysis was used to establish

petrophysical rock types for all the wells utilizing eight electric log curves. These petrophysical rock types were then cross-referenced with the core data. The result showed three main petrophysical rock types with a distinct reservoir quality for each one, namely; reservoir-rock (Rock 1), an intermediate rock type (Rock 2), and non-reservoir rock (Rock 3). Table 2 shows detailed descriptions of each rock type. Furthermore, univariate statistics of porosity for each rock type show clear separation between each class of porosity as indicated in the histograms shown in Fig. 6.

An attempt was made to build a 3D petrophysical rock model as defined at the wells but the resulting model (Fig. 7) has no geological character or meaning. Therefore it was decided to combine both the environment / depositional facies model built earlier, that is fully supported by the geologist with the petrophysical rock type model supported by the reservoir engineer, into a single integrated facies model. This was accomplished by distributing the petrophysical rock types defined at the wells within each environment of depositional facies separately. Fig 8 shows the resulting 3D model of petrophysical rock type distributions utilizing depositional environment facies model as regions.

Stochastic Seismic Inversion

A poststack amplitude inversion was performed on the 3D Hawtah seismic volume for the purpose of incorporating seismic impedance data into the 3D Hawtah model. That is, the available seismic data was transformed from wiggle trace information to acoustic impedance so as to be useful for influencing 3D reservoir descriptions. This transformation and integration explicitly considered that seismic-based information is an imperfect predictor of well impedance logs, and subsequently, an even less perfect predictor of facies.

Stochastic inversion has been employed in this study in place of the conventional deterministic approach which gives absolute impedance results with resolution dependent on the inherent seismic bandwidth. The stochastic inversion approach capitalizes on stochastic simulations such as Sequential Gaussian Simulation (sGs) including collocated cokriging to generate multiple, equi probable realizations of impedance pseudo-logs at each seismic trace location, and then to select the closest one to the actual seismic trace. Moreover, the stochastic inversion approach honors the constraining well impedance logs along with their vertical resolution as well as the specified univariate and bivariate statistics of impedance by area and/or zone.

Elements of the inversion processing of the Unayzah Reservoir included a simultaneous wavelet estimation and time-depth analysis, zero-phase broadband reflectivity processing, 3D forward modeling of low-frequency reflectivity balancing and impedance fields, deterministic inversion, and a high-frequency log-scale stochastic simulation of impedance constrained by the deterministic inversion. The result is an impedance model at the same scale of resolution as the well logs as shown on Fig 9.

A seismic horizon picked at top reservoir combined with time to depth relationships determined from log to seismic ties was used to convert the geologic model layering scheme to seismic micro-horizons within the reservoir, and to estimate the seismic wavelet.

Time to Depth Conversion of AI (Acoustic Impedance)

Reservoir modeling is carried out in the depth domain, which requires the conversion of seismic acoustic impedance (AI) from the time to the depth domain. The conversion can be done by simply snapping the impedance values between two markers, which are equivalent to the same depth markers, into a pre-defined 3D grid. In the case of the Unayzah model, the geological 3D reservoir grid model was defined in depth utilizing all the thirteen zones and an areal grid which covers the field outline. The total number of vertical cells (layers) is 133 with an areal grid of 162 in the x direction and 217 in the y direction (Fig. 10), making the model size more than 3 million cells in total. AI data between each of the 15 zones (which are available in time domain) were snapped to the corresponding 15 zones in depth. This conversion from one domain to another is considered as an implicit one, unlike the conventional velocity-based conversion. Fig. 11 shows a schematic diagram of how this was done.

Acoustic Impedance (AI) Porosity Relationship

Well data were thoroughly examined by means of univariate and bivariate analysis such as histograms and scattergrams respectively to look for systematic relationship between well AI and porosity. Fig 12 shows a cross plot of porosity and AI which indicated a large cloud of data with no strong relationship between these two variables. However, there was evidence of a strong AI and porosity relationship once the data was segregated by petrophysical rock type as shown in Fig. 13. This figure shows that the better the reservoir quality rock (Rock 1) the higher the correlation coefficient between porosity and AI. However, in the non-reservoir rock type (Rock 3), the relationship between the two variables is lost. As a result, facies modeling plays a major role in determining how much weight the seismic should have to influence the estimation of porosity in the inter well regions.

Porosity and Permeability Modeling

A 3D Porosity model was built using the high resolution impedance model and utilizing the proper correlation coefficient for each rock type as defined in the 3D petrophysical rock model built earlier. This was accomplished through the use of sequential Gaussian simulation (sGs) of porosity with collocated cokriging using acoustic impedance (AI) as soft data. Fig. 14 shows the resulting 3D model of facies specific porosity. The sequential Gaussian simulation was chosen for its ability to generate models of porosity which capture the heterogeneity of the reservoir as well as its power to generate multiple realizations of modeled porosity models which can be ranked for use with fluid flow simulation tools,

such as streamline simulation. In the case of the Unayzah Reservoir, only one realization of porosity was selected for fluid flow simulation for practical reasons.

Permeability curves were constructed for each well in the Hawtah Field honoring both the permeability thickness (Kh) from pressure buildups, flow meter profiles, and core permeability data. The flow profile is used to allocate the total or gross measurement of pressure buildup to a higher resolution permeability log. Fig 15 illustrates how flow meter data is used in allocating permeability logs which has the same scale and resolution as the flow meter profile. The newly produced permeability log is then integrated with core porosity and permeability data (Fig 16) for each facies to overcome the problem of missing data at non-perforated intervals of the well. The integration is accomplished by assigning permeability values from cloud transforms of core porosity and permeability as shown in Fig. 17. In non-perforated intervals, however, facies based cloud transforms are used to randomly sample possible permeability values from the core data for a given porosity class. A 3D correlated probability field was generated from the existing conditioned permeability logs at each well location. The correlated probability field is then used to sample the cloud transforms for each facies. For a given porosity value corresponding to the existing facies-based porosity model it then assigns a permeability value. The result is a permeability model that both honors the engineering data at the well location (permeability from pressure buildup and flow meter) and retains core porosity and permeability character for each facies. Stratification of the Unayzah Reservoir is captured better than using conventional techniques, as illustrated in Fig. 18, where thin layers of high permeability are retained in the model that would have otherwise been lost.

Conventional Porosity and Permeability Models

Two sets of porosity and permeability models were constructed using the interpolation methods of least squares and inverse distance and a linear transformation of porosity to permeability. Porosity was distributed between the wells using inverse distance for the same 3D gridded integrated framework. Fig 19 shows the inverse distance porosity model. This figure shows a very homogeneous porosity distribution, achieved by the inverse distance interpolation using only the well porosity data.

The permeability model was built by directly transforming this porosity model. A regression line was fitted through the cloud of core porosity and permeability values by averaging the distribution of permeability for a given porosity value. This linear relationship was then used to transform the porosity model. The resulting permeability model is unconstrained, with permeability model no actual permeability's at the well locations. Fig. 20 shows the resulting homogenous permeability distribution derived using this technique.

Fluid Flow Performance

In order to determine the level of accuracy between the two approaches and the advantage of data integration, fluid flow simulations were run. Several criteria were set to determine the level of accuracy, which included water breakthrough time, CPU time required to history match, and fluid flow movement pattern.

The simulation model was constructed using permeability, porosity, depth, cell thickness, and petrophysical rock types in the case of integrated model. No upscaling was done on either set of models to eliminate any inherent errors associated with upscaling. Relative permeability curves as well as capillary pressure curves were built as rock type specific to produce identified regions. Furthermore, the global porosity of the rock types were split into five bins for simulation modeling as shown on Fig. 21. Water injectors were placed at the down-dip ends of the structure while oil producers were placed at the structural high.

Water floods were modeled using a streamline simulator and the porosity and permeability distributions obtained from both the conventional approach and the integrated approach discussed in this paper. Quick-look water flood simulations provided water breakthrough times, fluid front behavior, and water cut comparisons. A detailed fluid flow simulation was also carried out using a finite difference simulation technique for both approaches to assess the required CPU time for history matching, and pressure and error analysis comparisons.

Results and Discussion

Each set of models when fed into fluid flow simulation produced very different flow results in terms of breakthrough times and fluid movement patterns. In the case of the integrated models, water had a preferred direction through thin zones of high permeability (Fig. 22) as captured by the stratification of the reservoir model which mimics the field data. By contrast, for the conventional approach the fluid front movement has no preferred direction throughout the model as shown on Fig. 23 because the conventional reservoir model is more homogenous compared to the integrated model. The computed water arrival time of the integrated model is a much closer match to the field data than that of conventional model as shown in Fig. 24.

The fluid flow simulation results seem to indicate a significant impact on level of accuracy in both history matching time and well performance. Fig. 25 shows the error analysis for each time step for both the conventional and the integrated model. The error at each time step for the integrated models are smaller and more stable than the errors from the conventional non-integrated model. Another advantage of the integrated approach is clearly seen in the improvement of simulation speed for every time step as shown in Fig. 26, with as much as 17% saving of computational time without changing the properties of the model. Other evidence of improvement when using the integrated approach is shown in Fig. 27, which compares calculated pressure values versus observed pressure. As shown in this figure, the calculated pressures from the integrated model simulation match the

observed pressure data well. Whereas the calculated pressures from the conventional model simulation overestimates the observed pressures by up to 25%.

Conclusion

A new technique or scheme for integrating data of diverse source and different scales has been presented. The added value of data integration has been demonstrated by the significant effect of the characteristics of the reservoir models generated. The integration of geological depositional facies data produced profound effects on the spatial distribution of petrophysical rock types between wells. Moreover, the incorporation of seismic acoustic impedance data provided additional information allowing the heterogeneity and small-scale variations in the inter-well regions to be captured in the model. The integrated method provided more realistic and meaningful models for the complex heterogeneity of the Unayzah Reservoir as compared to the homogenous results produced by the non-integrated conventional approach. Moreover, the effect of predictions of fluid-flow behavior was significant when using the integrated approach. Fluid flow movement patterns, breakthrough time, major reduction of CPU time and the pressure match with observed data are only few examples of the many advantages of the integrated approach described in this paper.

Acknowledgments

Authors would like to extend their thanks to Ministry of Petroleum and Minerals and Saudi Aramco for the permission to publish this paper. We also would like to thank the management of Saudi Aramco and University of Aberdeen for their support. We wish to thank the following colleagues at Saudi Aramco: Hassan AlKhaf, Maher Al-Marhoon, and Khalid Mashoug for their valuable contributions.

Reference

1. AlAli,Z, and Alqassab,H., 2000, Optimizing Simulation Models by Upscaling from Integrated Reservoir Models; A Case History. SPE 59448.
2. Alqassab, H., 1999, Constraining Permeability Field to Engineering Data: An Innovative Approach in Reservoir Characterization. Saudi Aramco Journal of Technology.
3. Alqassab, H., Heine,C., 1998, A Geostatistical Approach to Attribute Interpolation Using Facies Templates, An Advanced Technique in Reservoir Characterization. SPE 49449.
4. Araktingi, U., Bashore, W., 1992, Effects of Properties in Seismic Data on Reservoir Characterization and Consequent Fluid Flow-Predictions When Integrated With Well Logs. SPE 24753.
5. Araktingi, U., Bashore, W., Hewett, T., and Tran, T., 1990, Integration of Seismic and Well Log Data in Reservoir Modeling,. Presented at the Third Annual NIPER Conference on Reservoir Characterization, Tulsa, Oct. 5-7,1990.
6. Jones, D., AlAli,Z., AlKhalifa,M., Aktas, G., 1999, Development of a Conceptual Model for The Study Field, Saudi Arabia. An Internal Report.

Tables

Facies Type	Description
Dune	Medium to fine grained clean sandstones, well sorted, poorly cemented.
Interdune	Very fine to fine grained moderately argillaceous sandstones, horizontal to wavy laminated.
Lake Margin Sabkha	Very fine grained sandstone interlaminated with silty layers. Horizontal to wavy bedded.
Fluvial	Fine to coarse grained, poorly sorted sandstones, organized into sharp-erosive based upward-fining package.
Lacustrine	Variable silty mudstones, present in varying thickness, most commonly at the base of upward-drying cycles.

Table 1 Description of Depositional Environment Facies.

Rock Type	Description
Rock 1	Well sorted, medium to coarse grain sandstone. Connate water saturation of less than 10% and gamma ray of less than 30 API units.
Rock 2	Fine to medium grain silt sandstone. Gamma ray between 30-45 API units.
Rock 3	Fine grained siltstone. Gamma ray greater than 45 API units with high connate water saturation.

Table 2 Description of Petrophysical Rock Types.

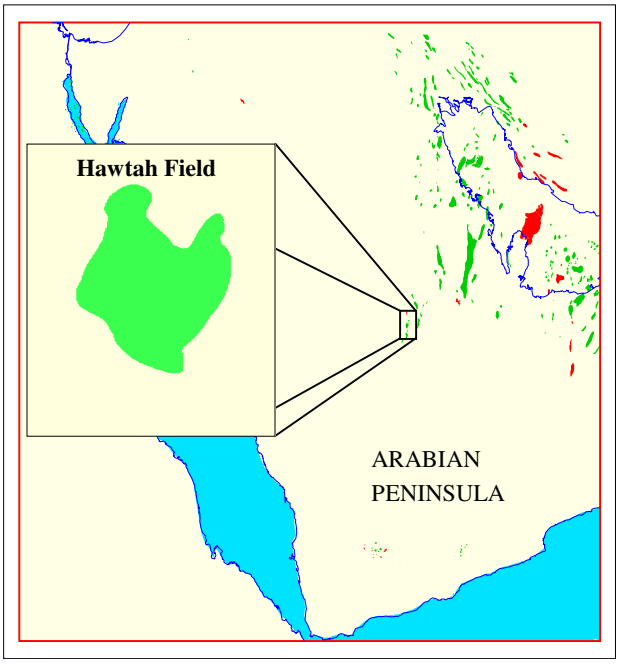

Figure 1 Location Map of Hawtah Field.

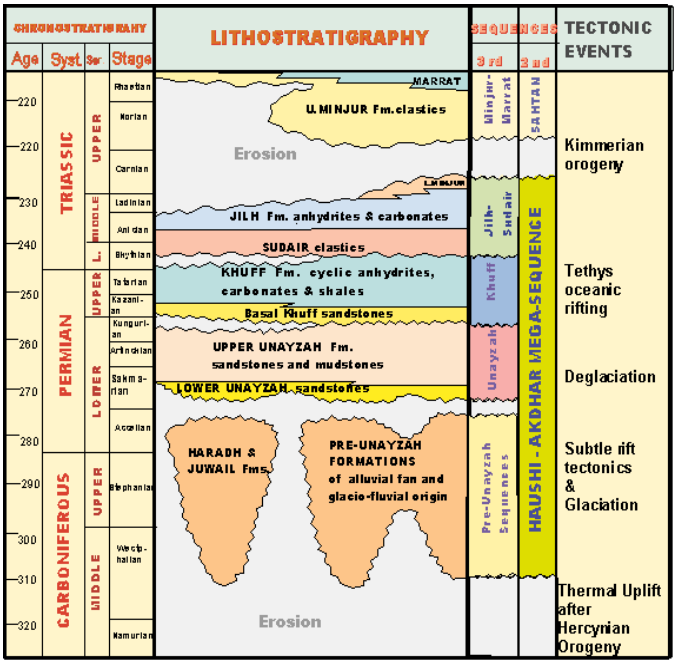

Figure 2 Unayzah Stratigraphic Chart.

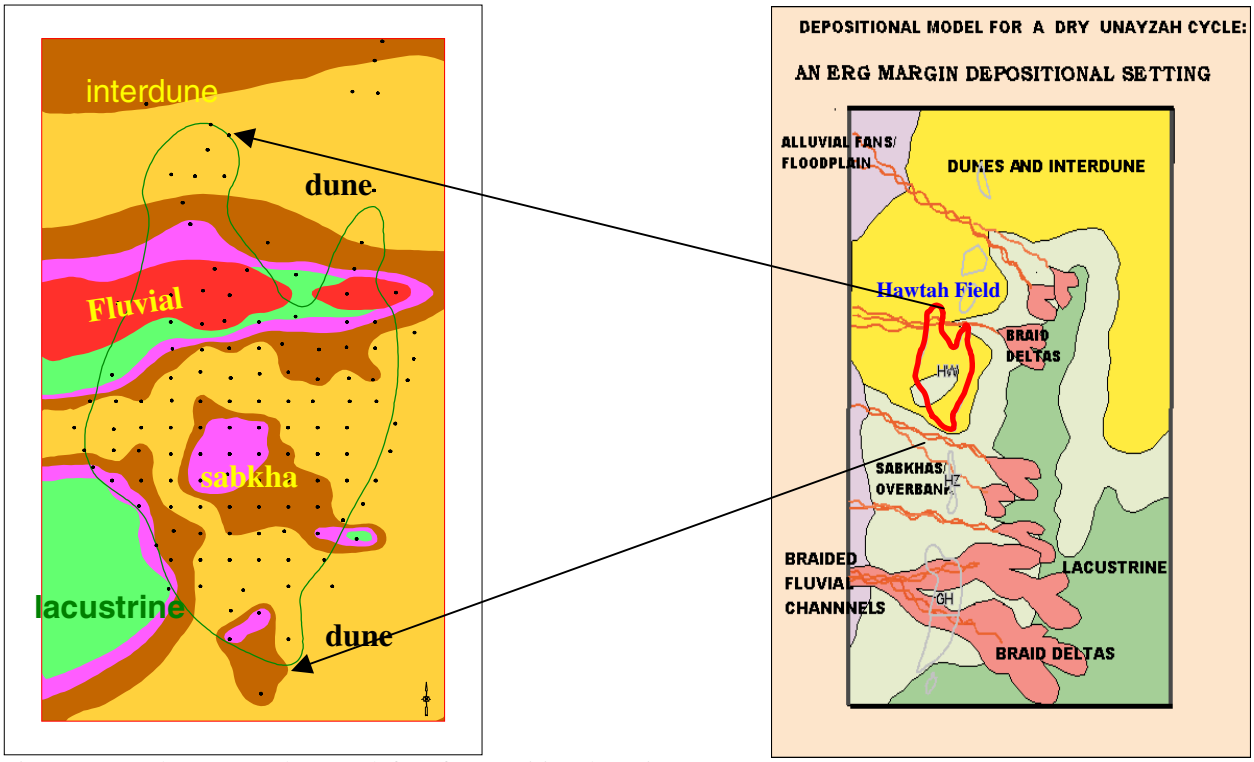

Figure 3 Hand Contoured Map (left) of Depositional Facies Using Well Data and Regional Depositional Setting (Right).

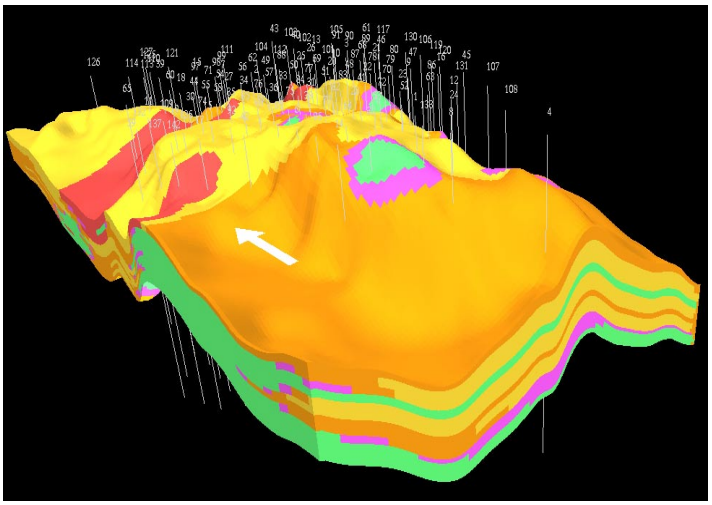

Figure 4a Stacked Depositionl Environment Facies Maps for the 13-zones.

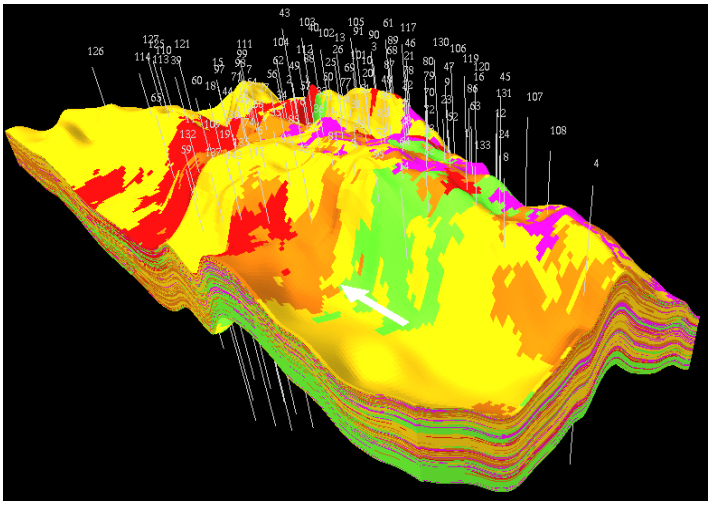

Figure 4b 3D Model of Depositional Environment Facies.

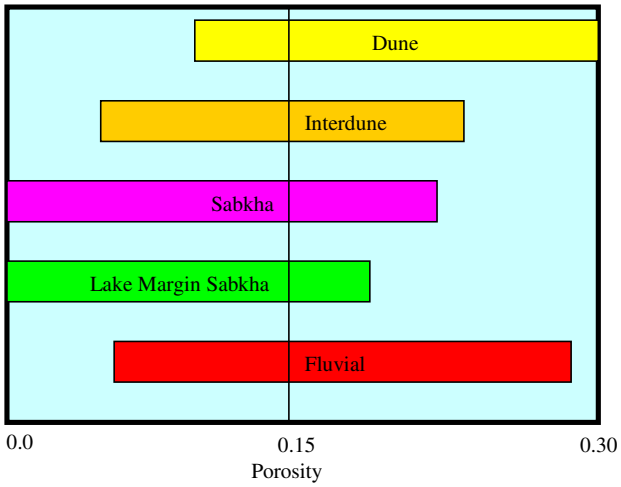

Figure 5 Porosity Ranges of Depositional Environment Facies.

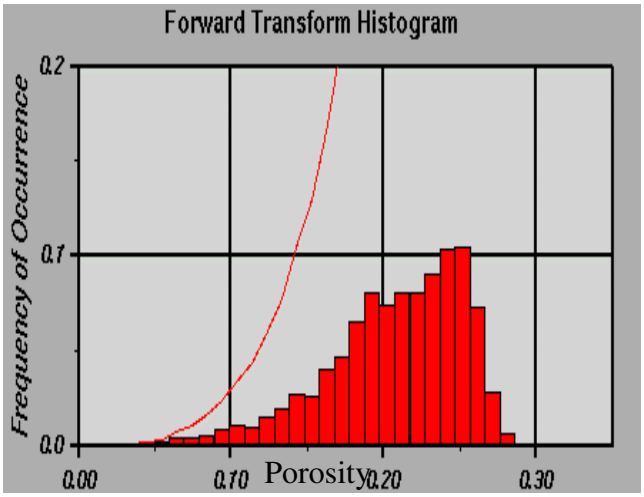

Figure 6a Porosity Distribution of Petrophysical Rock 1 Type.

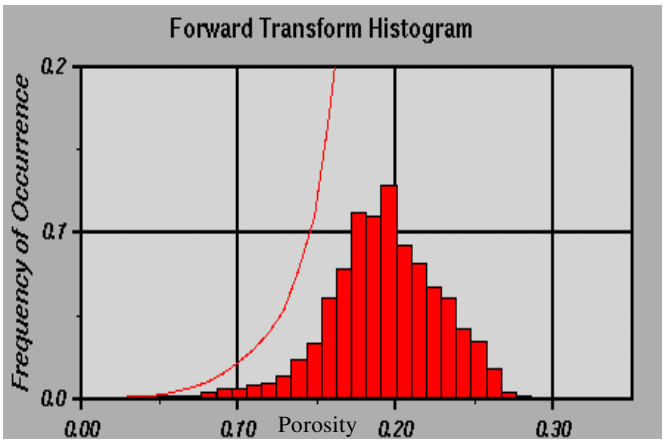

Figure 6b Porosity Distribution of Petrophysical Rock 2 Type.

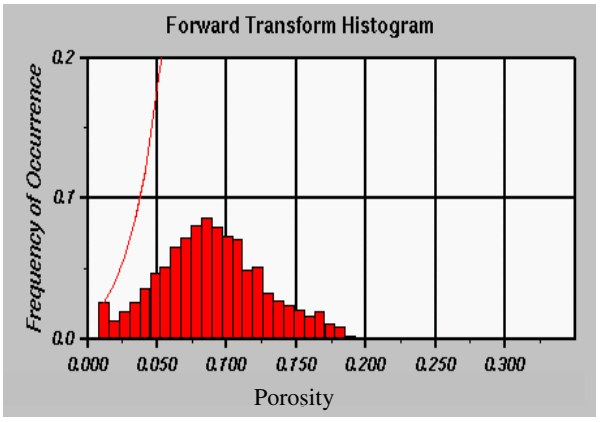

Figure 6c Porosity Distribution of Petrophysical Rock 3 Type.

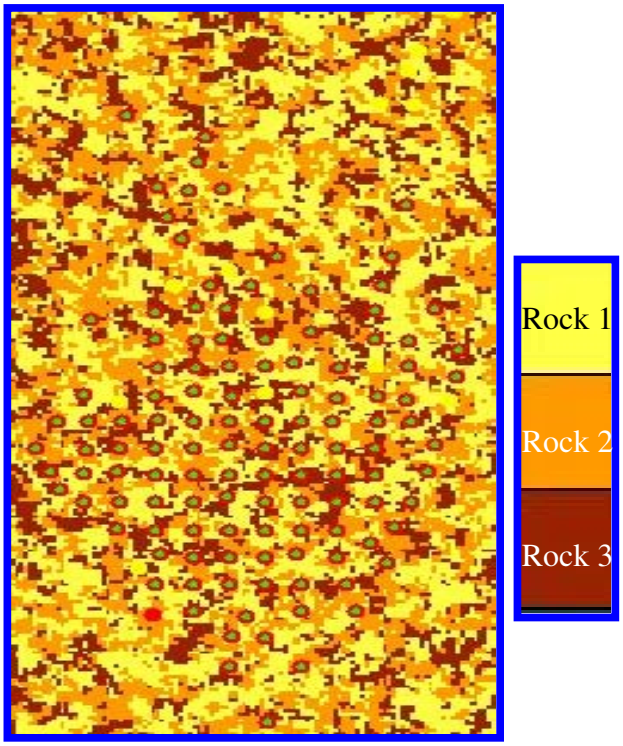

Figure 7 A Slice of the Petrophysical Rock Types Model.

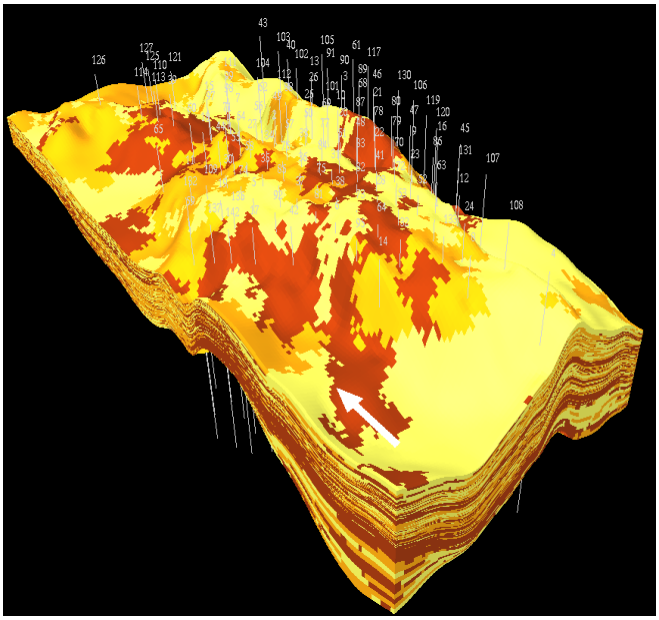

Figure 8 Petrophysical Rock Type Model Using Rock Types Defined at Wells and Environment of Depositional Facies Model as Regions.

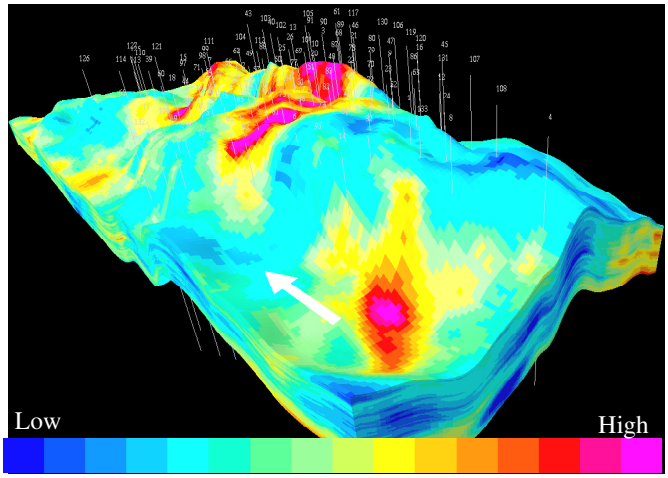

Figure 9 High Resolution Seismic Impedance Model as a Product of Stochastic Inversion.

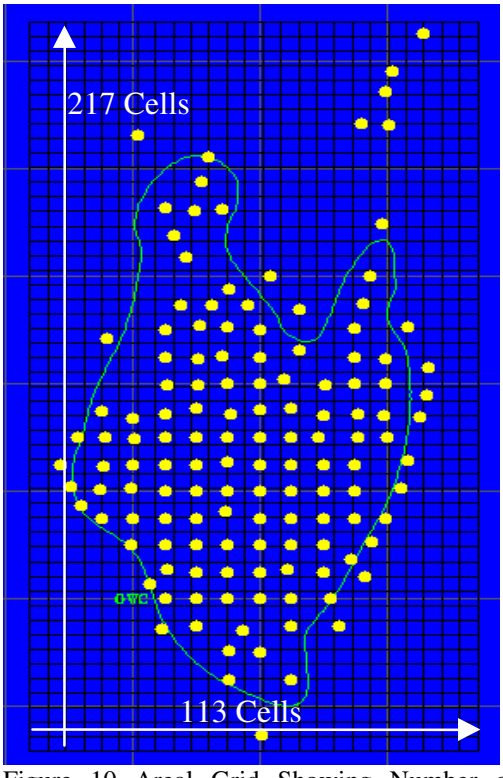

Figure 10 Areal Grid Showing Number of Cells in X-Direction and Y-Direction.

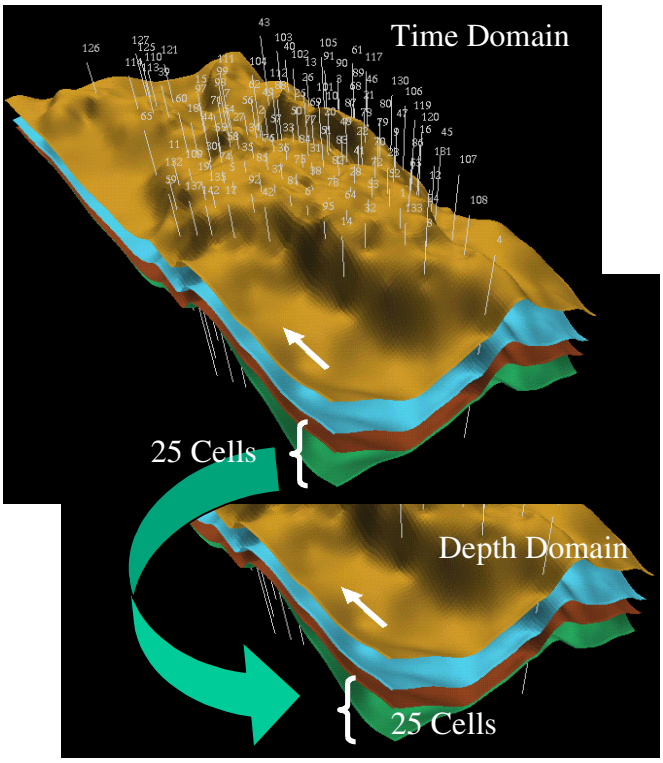

Figure 11 Schematic Diagram Showing Time (Top) to Depth (Bottom) Conversion. The 25 Cells are Snapped Between Two Equivalent Markers.

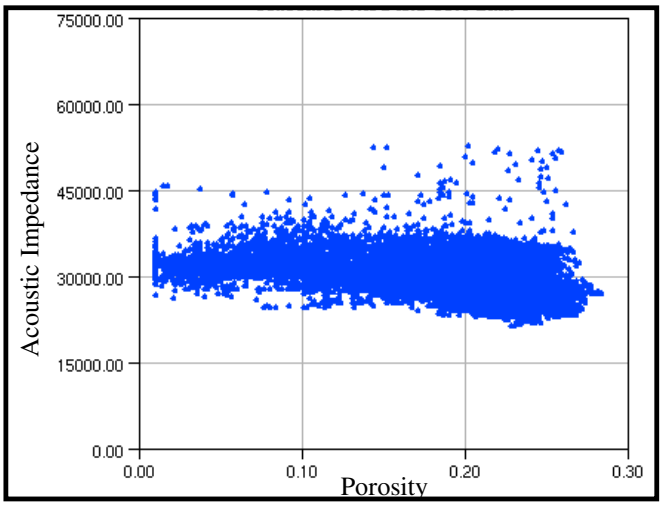

Figure 12 Cross Plot of Well Porosity (X axis) and AI (Y axis) for the Entire Reservoir.

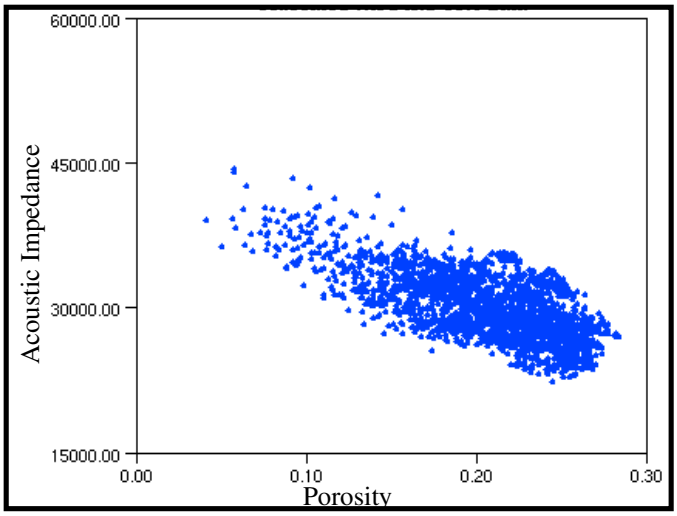

Figure 13a Cross Plot of Well Porosity (X axis) and AI (Y axis) for Rock 1 Type.

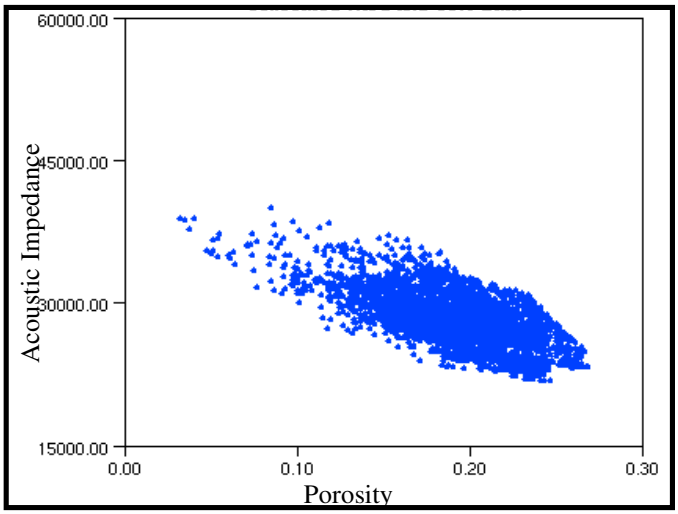

Figure 13b Cross Plot of Well Porosity (X axis) and AI (Y axis) for Rock 2 Type.

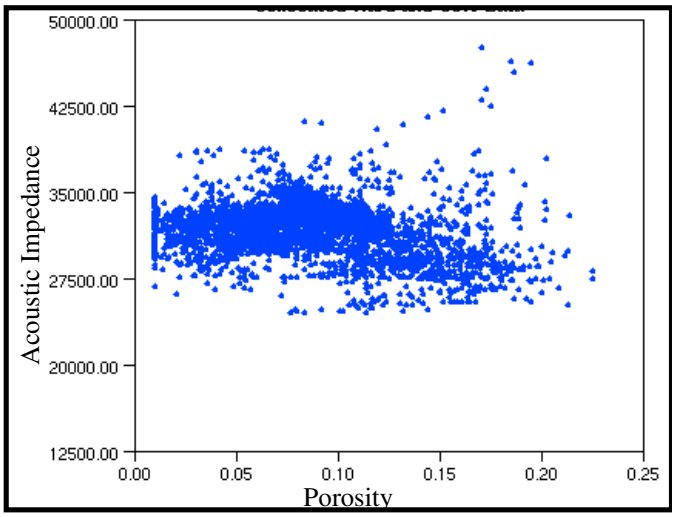

Figure 13c Cross Plot of Well Porosity (X axis) and AI (Y axis) for Rock 3 Type.

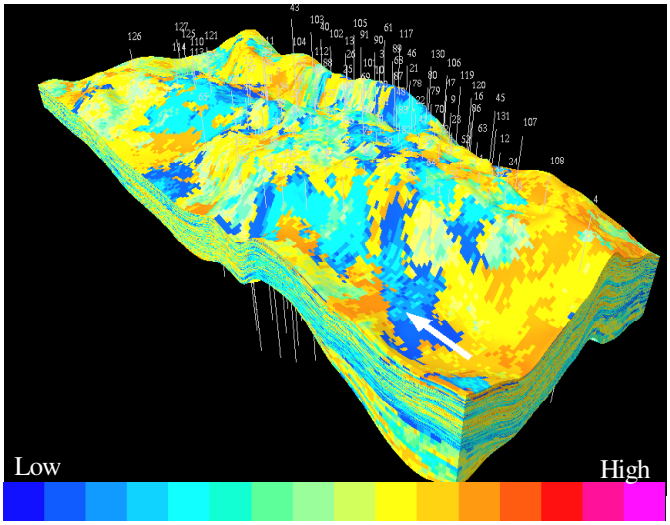

Figure 14 3D Rock Specific Porosity Model Using sGs with Collocated Cokriging.

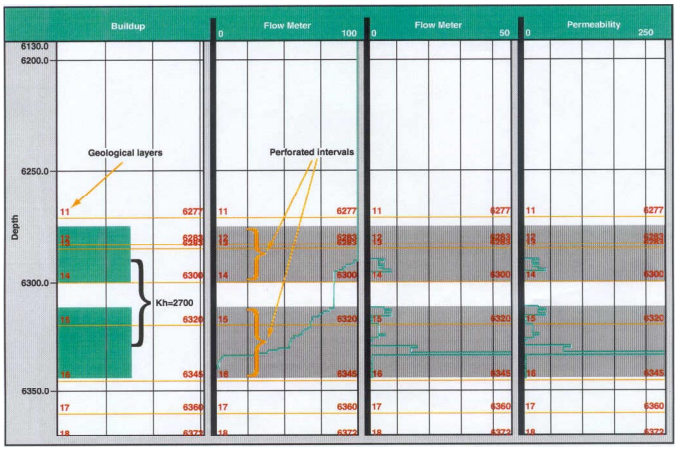

Figure 15 Permeability Thickness (Kh) Allocated by Flow Meter Profile in One of Hawtah Field Wells.

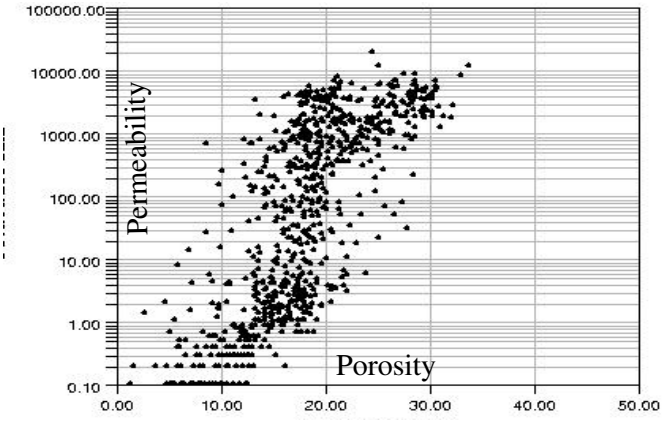

Figure 16a Cross Plot of Core Porosity and Permeability for Petrophysical Rock 1 Type.

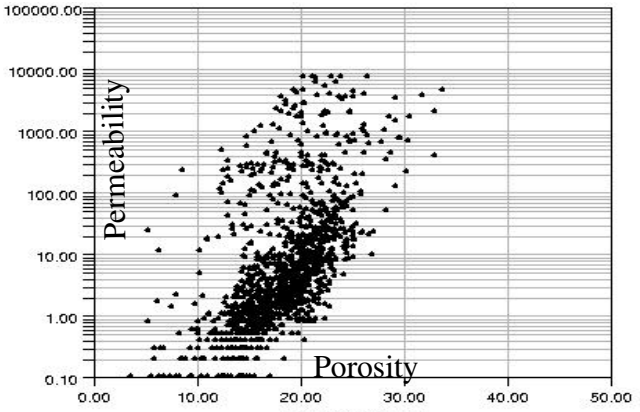

Figure 16b Cross Plot of Core Porosity and Permeability for Petrophysical Rock 2 Type.

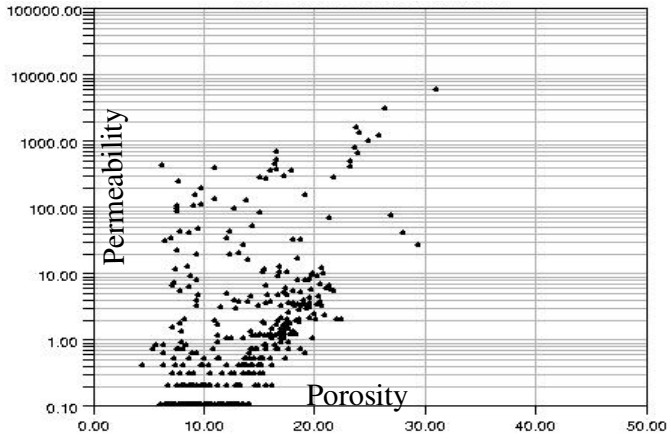

Figure 16c Cross Plot of Core Porosity and Permeability for Petrophysical Rock 3 Type.

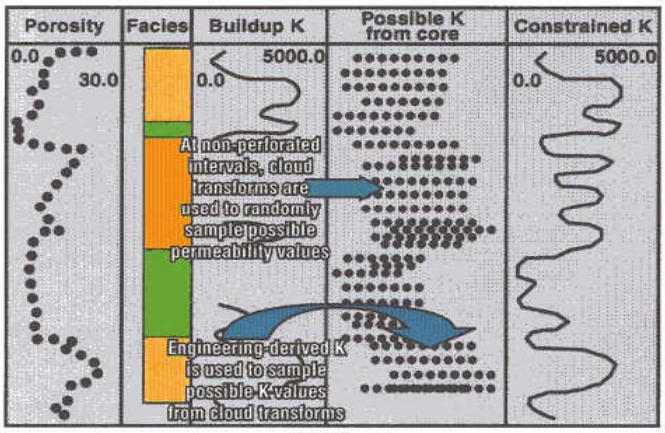

Figure 17 Integrating Buildup Permeability As Selecting Criteria in Sampling a Range of Permeability Values from Core Data.

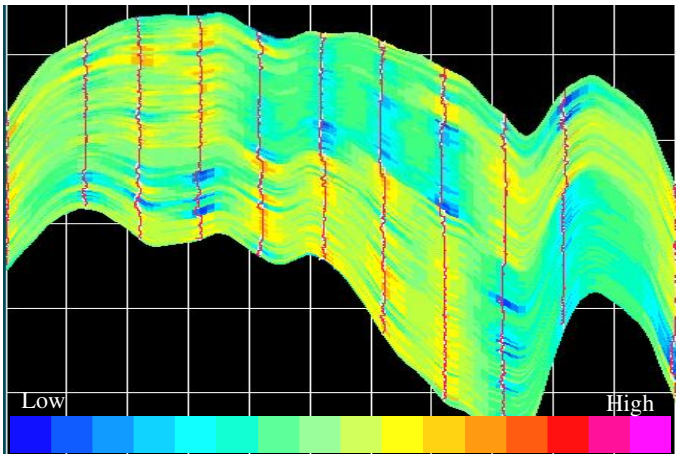

Figure 19 Porosity Model Using Inverse Distance Approach.

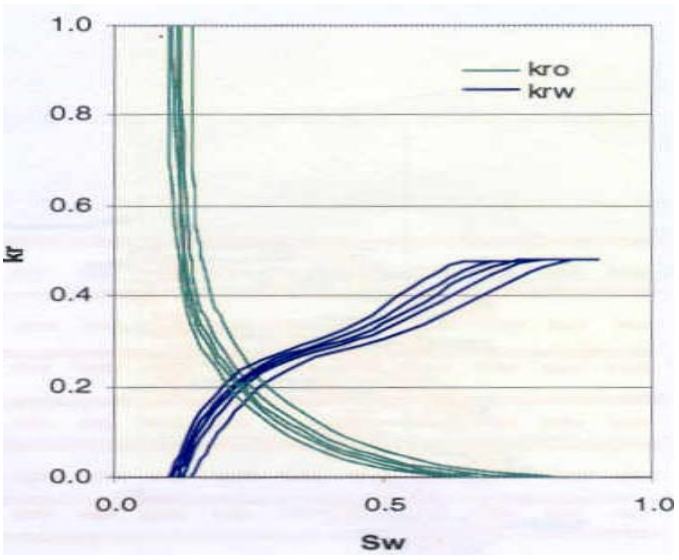

Figure 21An Example of Relative Permeability Curves for Rock 1 Type with Five Porosity Bins.

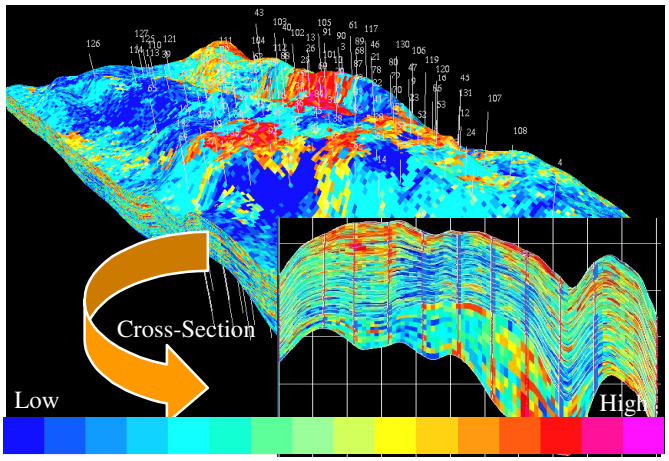

Figure 18: 3D Permeability Model Using Core, Engineering, and Seismically Constrained Rock Specific Porosity Model.

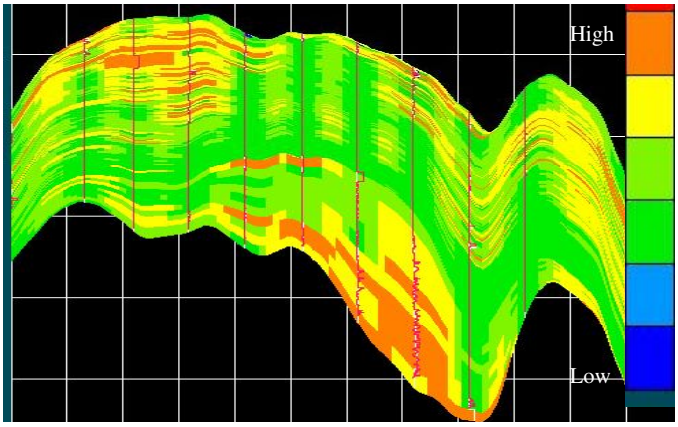

Figure 20 Permeability Model Using Linear Transformation of Porosity to Permeability.

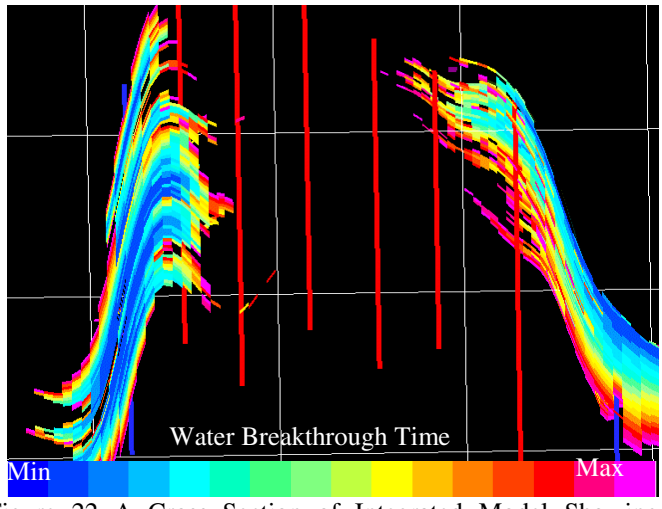

Figure 22 A Cross–Section of Integrated Model Showing Water Breakthrough Time. Note the Stratification (Right) of the Reservoir.

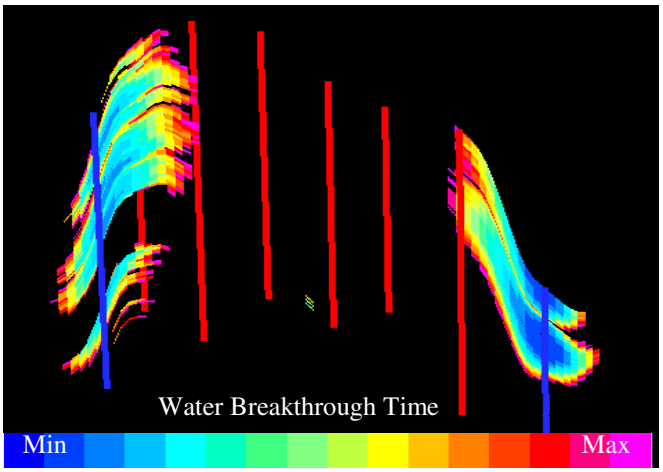

Figure 23 A Cross–Section of Conventional Model Showing Water Breakthrough Time. Note the Uniform Fluid Front (Right) of the Reservoir.

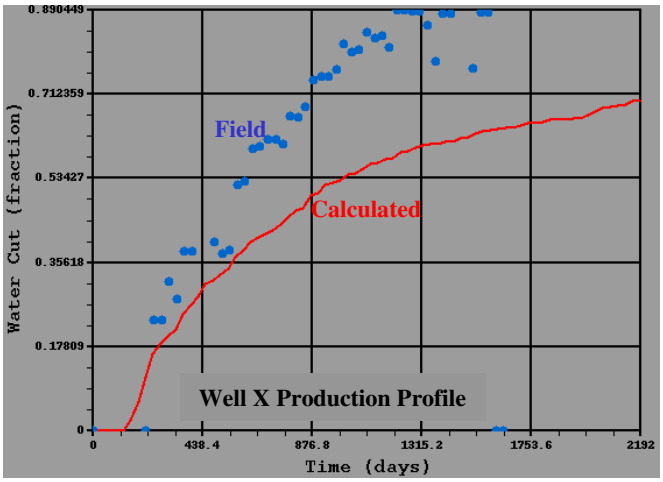

Figure 24a Water Cut of Integrated Model. Note the Water arrival Time as Compared to Field Date.

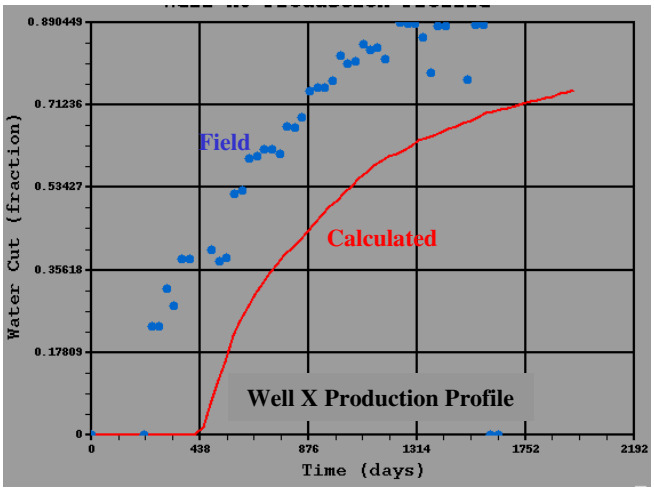

Figure 24b Water Cut of Conventional Model. Note the Water Arrival Time as Compared to Field Date.

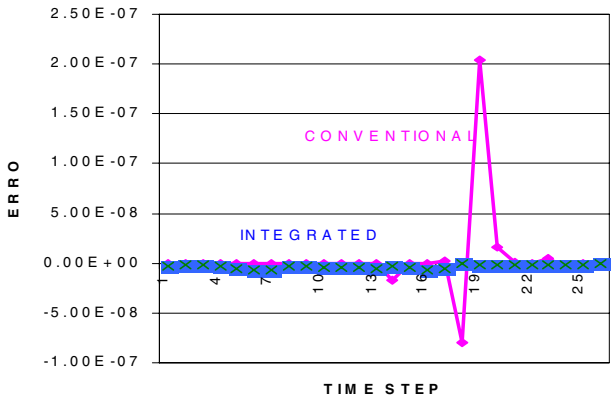

Figure 25 Error Plot Analysis for Each Time Step for Both Approaches.

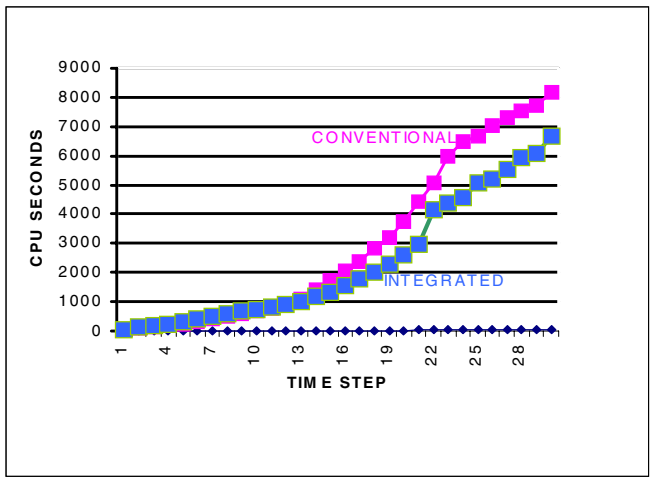

Figure 26 Comparison of the Two Approaches in Terms of CPU Time.

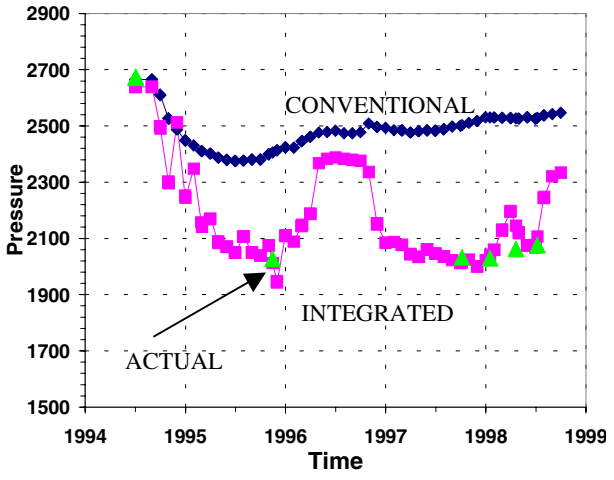

Figure 27 Pressure Match Comparison Between Both Types of Approaches.